Final Technical Report

on

Superfluid Helium Dynamics

Grant NAG5-1031

by

Steven W. Van Sciver
Principal Investigator
Professor
Nuclear Engineering & Engineering Physics
University of Wisconsin

January 15, 1990 - December 31, 1990

paper CD-4: 1991
Cryogenic Engineering
Conference. Huntsville, AL

CHARACTERIZING HE II FLOW THROUGH POROUS MATERIALS USING COUNTERFLOW DATA

J. R. Maddocks and S. W. Van Sciver,

University of Wisconsin, Madison,
Applied Superconductivity Center,
Madison, Wisconsin

ABSTRACT

Proposed space applications, such as the cooling of infrared and x-ray telescopes, have generated substantial interest in the behavior of He II flowing in porous materials. For design purposes, classical porous media correlations and room temperature data are often used to obtain order of magnitude estimates of expected pressure drops, while the attendant temperature differences are either ignored or estimated using smooth tube correlations. A more accurate alternative to this precedure is suggested by an empirical extension of the two fluid model. It is shown that four empirical parameters are necessary to describe the pressure and temperature differences induced by He II flow through a porous sample. The three parameters required to determine pressure differences are measured in counterflow and found to compare favorably with those for isothermal flow. The fourth parameter, the Gorter-Mellink constant, differs substantially from smooth tube values. It is concluded that parameter values determined from counterflow can be used to predict pressure and temperature differences in a variety of flows to an accuracy of about ±20%.

INTRODUCTION

A general interest in the behavior of He II flowing through porous materials stems from recent space based technological applications, which require the management of He II in a weightless environment. Specific applications include; fine mesh screens and light weight, high porosity ceramics for fluid acquisition devices,[1] sintered metal or packed metal powders for use as porous venting plugs[2,3] and very fine pore packed powders or ceramics to be used as superleaks.[4,5]

For design purposes, the Darcy permeability of a specific porous sample, measured at room temperature, is often used to obtain order of magnitude estimates of expected pressure drops. Expected temperature differences are either neglected or estimated using the Gorter-Mellink relation and smooth tube values of the Gorter-Mellink parameter. However, experiments show that the major portion of the pressure drop

in high porosity ceramics results from kinetic energy losses rather than viscous drag losses due to laminar flow. In addition, the superfluid losses are not generally negligable. The result is that room temperature measurements of the permeability do not provide adequate pressure loss estimates.

Through a set of experiments discussed in the present paper we show that a better method of characterizing porous media for He II applications involves a straightforward measurement of counterflow heat transport. These results combined with knowledge of the porous media appear to allow the prediction of temperature and pressure gradients through the medium to within ± 20%.

GOVERNING EQUATIONS

The equations most commonly used to analyze the behavior of He II in simple one dimensional geometries are:

$$\rho_s (Dv_s/Dt) = -\nabla P_s - F_s - F_{sn}, \tag{1}$$

and

$$\rho_n (Dv_n/Dt) = -\nabla P_n + \eta_n \nabla^2 v_n - F_n + F_{sn}, \tag{2}$$

where

$$\nabla P_s = (\rho_s/\rho)\nabla P - \rho_s s \nabla T, \tag{3}$$

$$\nabla P_n = (\rho_n/\rho)\nabla P + \rho_s s \nabla T. \tag{4}$$

The empirical forces F_n, F_s and F_{sn} are added to account for the effects of normal fluid turbulence, superfluid turbulence and mutual friction respectively.

To formulate the equations of motion in a way that is applicable to porous materials, the following functional forms are assumed. Based on a previous experiment[6] it is assumed that,

$$F_n = b_n \rho_n v_n^2, \tag{5}$$

$$F_s = b_s \rho_s v_s^2. \tag{6}$$

It is further assumed that the Gorter-Mellink relationship describes the mutual friction, so that

$$F_{sn} = A(T)\rho_s \rho_n (v_s - v_n)^3. \tag{7}$$

Finally, the empirical Darcy law,

$$\nabla P = -\eta(v/k), \tag{8}$$

is used to replace the laminar term $(\eta_n \nabla^2 v_n)$ in equation (2), where k is the Darcy permeability.

Each term in equations (1) and (2) is replaced by its appropriate functional form. Steady state conditions are assumed, so the time derivatives are set equal to zero, and the equations then reduce to:

$$\nabla P_s = -b_s \rho_s v_s^2 - A(T)\rho_s \rho_n (v_s - v_n)^3 \quad (9)$$

$$\nabla P_n = -(\eta_n/k)v_n - b_n \rho_n v_n^2 + A(T)\rho_s \rho_n (v_s - v_n)^3. \quad (10)$$

The present experiment is designed to test the appropriatness of this empirical model.

MATERIALS, APPARATUS AND PROCEDURE

The porous material used in the present experiment is a fibrous ceramic of the type used for heat shields on the space shuttle. The fibers consist of 78% silica and 22% aluminum borosilicate. The material is manufactured by Lockheed,[7] using a process which results in an inhomogeneous and anisotropic final product. It is available in a number of packing densities. Samples of 6 and 16 lbs/ft^3 are tested in the present experiment. The porosity (ε) of each sample type, determined as $\varepsilon = 1 - (\rho_{sample}/\rho_{fiber})$, is listed in Table 1.

The test section, shown schematically in figure 1, contains two symmetrically mounted samples separated by approximately 10 mm. It is configured as such to allow a broader study including isothermal flow and combined flow.[8] Within the test section, the samples are mounted in thin wall stainless steel tubing, to minimize parallel heat conduction paths. Heat conduction through the ceramic samples may be neglected, because the thermal conductivity of the sample material is at least six orders of magnitude smaller than that of He II. To insure that the samples fit tightly, they are carefully cut using a sharpened piece of the same stainless tubing in which they are mounted. The outer surface of the samples is lightly covered with vacuum grease, to ensure their ridgid placement duing experimentation. The room temperature permeabilities of several samples are carefully measured using helium gas, and two closely matched samples are selected and mounted in the test section.

A 110 Ω metal film resistor serves as a heater and is located between the samples. Allen-Bradley carbon resistors serve as thermometers. As indicated in figure 1, there are three thermometers, each located in the liquid. One between the samples and one approximately 2 mm outside each sample. They provide an absolute temperature resolution of ±0.5 mK. Temperature differences across the samples are determined by subtracting the absolute temperatures measured on either side of the samples. Finally, pressure drops across each sample are measured

Table 1. Comparison of the permeability and the coefficient b_n

sample	porosity	k_{gas}	k_{iso}	k_{cf}	$(b_n)_{iso}$	$(b_n)_{cf}$
		$m^2 \times 10^{11}$			m^{-1}	
6#	.96	5.7	22	8.5	8600	7300
16#	.90	2.9	10	3.5	13200	11500

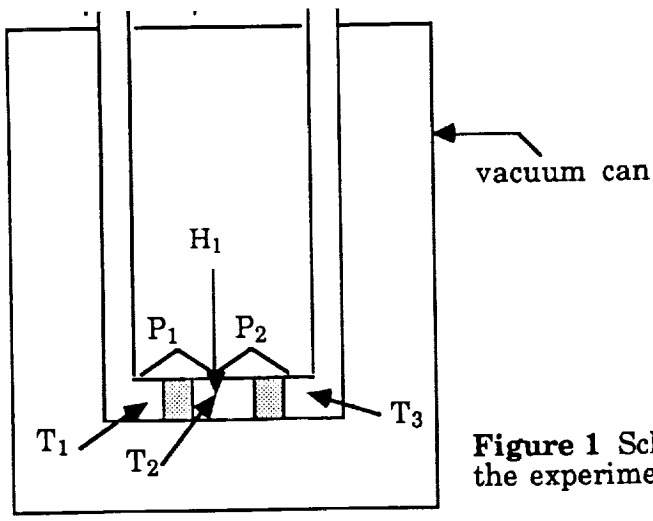

Figure 1 Schematic representation of the experimental apparatus.

using Siemens KPY-33R pressure sensors. These sensors have a nominal full scale range of 10 kPa and are mounted differentially. Their resolution is ±1 Pa.

All data are taken in the steady state with the aid of a Masscomp computer and associated periferals. The two pressure sensors, and the bath temperature are sampled sequentially at a burst rate of 1 MHz. This sequential sampling is repeated 25 times per second, for 32 seconds. The digitized data are then averaged to give a steady-state value.

During a somewhat longer but overlapping time period, the carbon resistance thermometers are sampled. The thermometers are sampled in sequence, each for a period of 10 seconds, at a sampling frequency of 6 Hz. This sampling frequency is determined by an A.C. conductance bridge, which is used to read the output of the thermometers. The bridge is a null device that gives a four-wire measurement of the conductance, by providing a 300 mV, 24 Hz excitation voltage.

EXPERIMENTAL RESULTS

For the purpose of data analysis, it is assumed that any effects due to mismatched samples can be neglected, so that half the heat deposited between the samples flows through each sample. Thus the relation

$$v_n = q/(2\rho s T A \varepsilon) \tag{11}$$

is used to determine v_n, where q is the total heat deposited, A the cross sectional area and ε the porosity.

While it is expected that this assumption will not cause a great deal of error in the analysis, it means that small differences in permeability (k), b_n, b_s and A(T) will not be measureable, as a result of the fixed boundary conditions.

A pressure gradient is always observed to accompany the flow of heat through He II in a narrow channel or porous material. The expected form of the pressure drop is given by the sum of equations (9), and (10) as

$$\nabla P = -(\eta/k)v_n - [b_n - (\rho_n/\rho_s)b_s]\,\rho_n v_n^2, \tag{12}$$

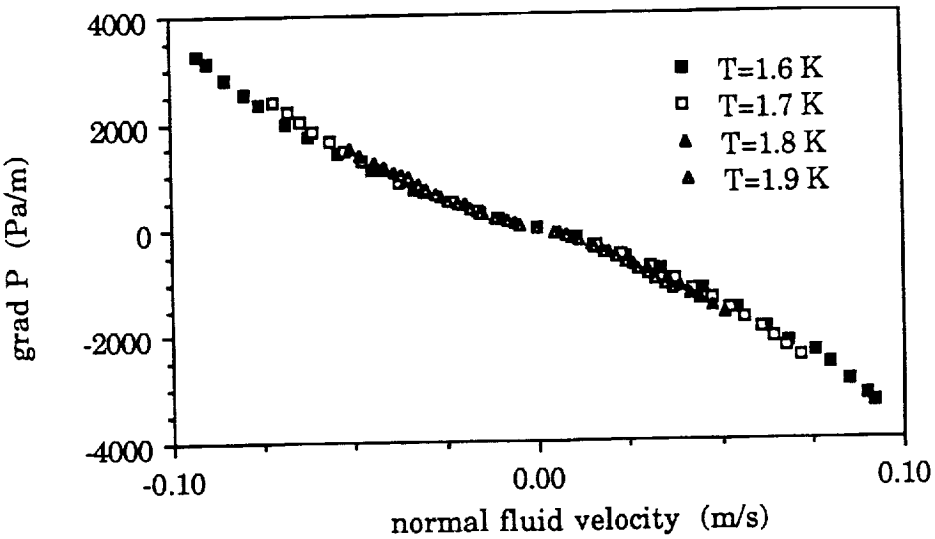

Figure 2 Velocity dependence of the pressure gradient, as a function of the temperature, for the 6# samples.

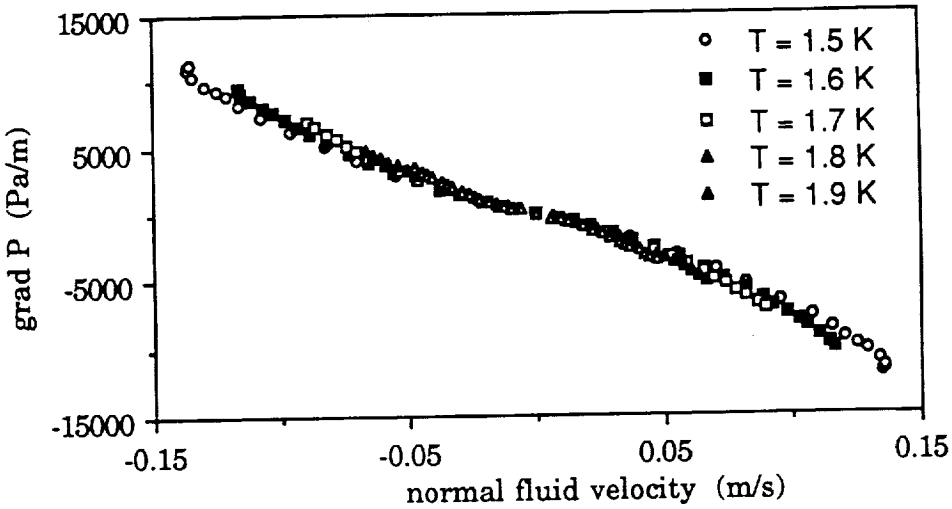

Figure 3 Velocity dependence of the pressure gradient, as a function of the temperature, for the 16# samples.

where the counterflow condition, $v_s = -(\rho_n/\rho_s)v_n$, has been used.

Figures 2 and 3 are plots of pressure gradient versus normal fluid velocity for the 6# and 16# samples. It is evident in both figures that the linear relationship between ∇P and v_n breaks down at normal velocities in excess of approximately 10 mm/s. This shows that the Allen and Reekie rule does not apply, even if modified to use the Darcy law for porous materials. In addition, the pressure gradients in figures 2 and 3 exhibit a small but definite temperature dependence. In order to determine if this temperature dependence is predictable, equation (12) is rewritten in the form

$$\nabla P/v_n = -\alpha(T) - \beta(T)v_n \qquad (13)$$

where, $\alpha(T) \equiv \eta/k$ and $\beta(T) \equiv \{b_n - (\rho_n/\rho_s)b_s\}\,\rho_n$.

Theoretically, the permeability can be determined from a plot of $\alpha(T)$ versus η_n. Practically, however, there is a large amount of scatter in $\alpha(T)$ because the pressure drop at low velocities, where laminar flow dominates, is not much larger than experimental resolution. Therefore, the permeability is determined using average values of $\alpha(T)$ and η_n. The permeabilities measured in this fashion are recorded in Table 1 and agree reasonably well with those measured in room temperature gas flow experiments. Agreement with isothermal permeabilities is not as good, but this may be due to the method used to obtain isothermal flow.[8]

In figure 4, the temperature dependence of the quadratic term, $\beta(T)$, is compared to that predicted by equation (12). The figure shows little sign of the expected temperature dependence, though clearly, $\beta(T)$ is affected by temperature. A plot of $\beta(T)$ versus ρ_n is shown in figure 5. The relationship is reasonably linear for both sets of samples, implying that the pressure gradient should be more accurately given by

$$\nabla P = -(\eta_n/k)v_n - b_n\rho_n v_n^2. \qquad (14)$$

Equation (14) is the expected normal fluid contribution to the pressure gradient, and seems to imply that the superfluid contribution is negligable, if not non-existent. Values of b_n, based on equation (14), are included in Table 1, as are values of b_n determined in isothermal flow.[8] The two measurements agree fairly well.

While equation (14) implies that the parameter b_s is not measureable in this experiment, it turns out that it is still possible to estimate it. Isothermal flow measurements[6,8] from two separate experiments, using similar materials, indicate that a reasonable estimate is given by $b_n = 2b_s$. Even though this relationship has been tested to a very limited extent, it

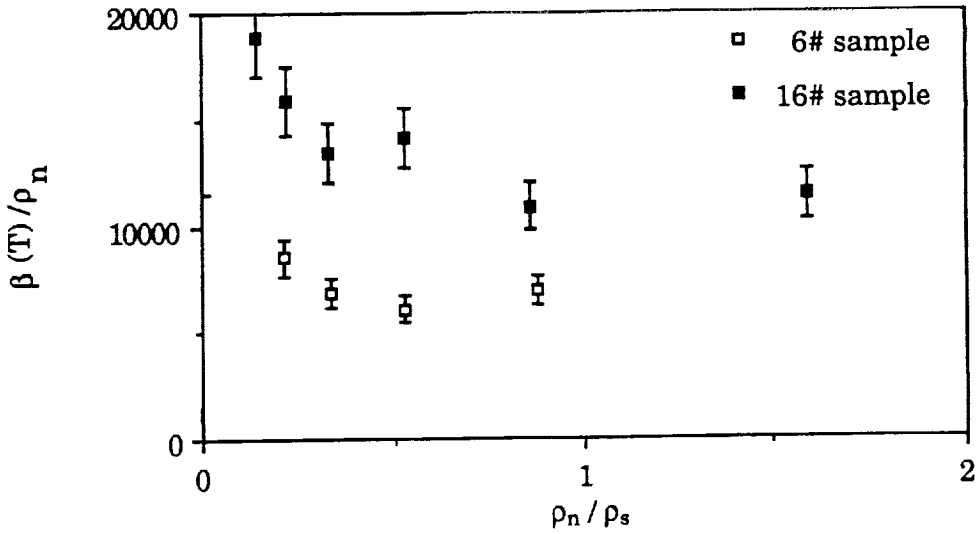

Figure 4 Temperature dependence of the quadratic coefficient $\beta(T)$ as given by equation (12).

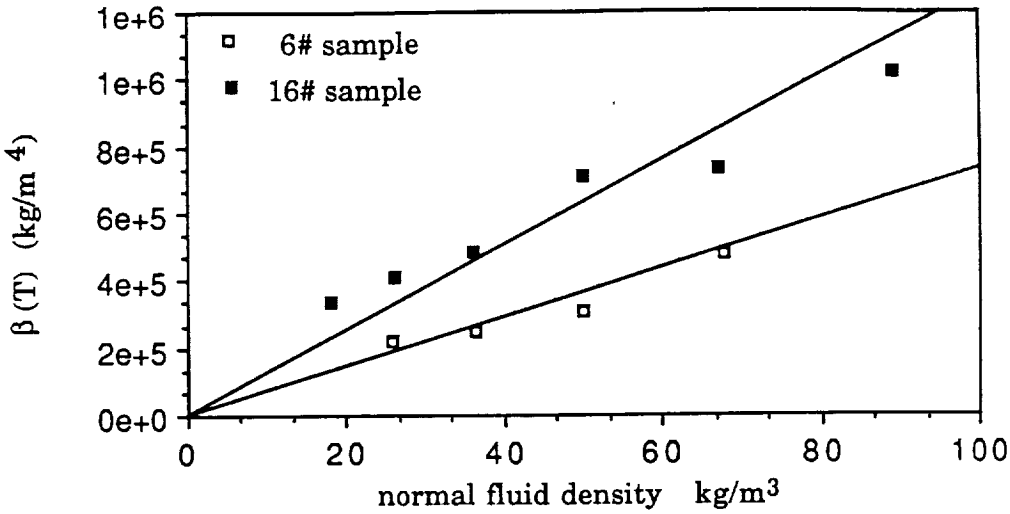

Figure 5 The temperature dependent, quadratic coefficient, β(T), as a function of rn only. The solid lines represent least square fits that have been forced through zero.

nonetheless makes it possible to obtain all the necessary parameters for calculating pressure drop from simple counterflow measurements.

When considering temperature data, the term F_s in equation (14) can, apparently, be ignored. However, the pressure gradient term is often less than one order of magnitude smaller than F_{sn}, so that, in general, it must be included. Equation (9) can be rearranged, then, to solve for F_{sn}, giving

$$\rho s\nabla T - \nabla P = A(T)\rho_n\rho(v_s-v_n)^3. \qquad (15)$$

Graphic solutions for A(T) are obtained from equation (15) by plotting the left hand side versus $(v_s-v_n)^3$. Values of A(T) as a function of temperature are plotted in figure 6, for both the 6# and 16# samples. The uncertainty in those values is on the order of ±100 m/s kg. For reference, a sample of the Gorter-Mellink coefficient for smooth tubes is included,[9] as well as A(T) calculated for the exit channels of the test section. The values of A(T) from the exit channels agree fairly well with the smooth tube results. In contrast, the values of A(T) for the porous samples are 2 to 4 times larger than smooth tube results, though the temperature dependence remains approximately the same. In addition, there appears to be some dependence on geometry.

Suprisingly, the 16# material shows less deviation from smooth tube results than does the 6# material. This result is opposite to what would be expected and remains unexplained. However, given the dramatic differences in geometry between porous media and smooth tubes, the relatively small variation of A(T) from smooth tube values of the Gorter-Mellink coefficient may imply that any geometry dependence of the parameter is very weak. In porous materials such as those considered in the present experiment, very large surface area to volume ratios and tortuous flow paths may give rise to inertial and path length effects.

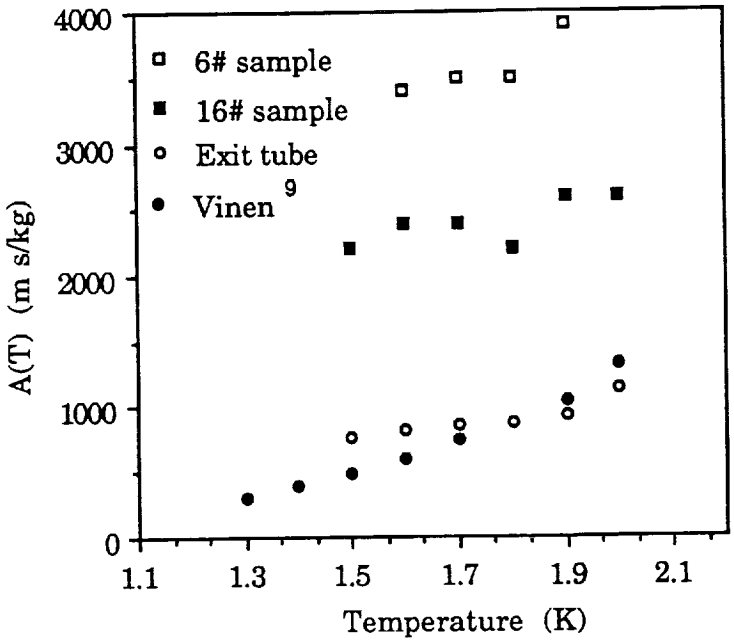

Figure 6 A plot of the Gorter-Mellink constant as a function of temperature, for both 6# and 16# samples

These effects may, in turn, account for why the parameter A(T) differs from measurements in smooth tubes.

CONCLUSIONS

The parameters necessary to estimate pressure and temperature gradients resulting from the flow of He II in high porosity ceramics can all be determined in counterflow. This approach offers a more accurate method of characterizing these materials for design purposes. Experimental results indicate that gradients can be predicted within 20%. Since counterflow experiments are relatively straightforward, it seems reasonable to suggest that they will provide a good and relatively easy characterization of any porous media.

ACKNOWLEDGEMENTS

Work supported in part by NASA/Goddard Space Flight Center under grant NAG-5-1031.

REFERENCES

1. M.J. DiPirro, Cryogenics, 30:193 (1990).
2. H. Rudiger and M. Wanner, Cryogenics, 27:38 (1987).
3. H. Nakai, and M. Murakami, Cryogenics, 27:442, (1987).
4. R. Srinivasan and A Hofmann, Cryogenics, 25:641, (1985).
5. G.L. Mills and A.R. Urbach, Cryogenics, 30:206, (1990).
6. J.R. Maddocks and S.W. Van Sciver, in: "Advances in Cryogenic engineering," Vol. 35A, Plenum Press, New York, (1990), p. 189
7. Lockheed Missles & Space Co. Inc., Astronautics Div. Sunnyvale, Ca.
8. J.R. Maddocks, "Transport Properties of He II flowing Through Porous Materials," PhD. Thesis, University of Wisconsin-Madison, Madison, Wisconsin (1991).
9. W.F. Vinen, Proc. Roy. Soc. (London), A240:114 (1957).

paper CD-21: 1991
Cryogenic Engineering
Conference. Huntsville, AL

THERMAL BEHAVIOR OF THE SHOOT GALLERY ARM

J.A. Nissen* and S.W. Van Sciver
Applied Superconductivity Center
University of Wisconsin
Madison, Wisconsin 53706

ABSTRACT

The planned Superfluid Helium On-Orbit Transfer (SHOOT) experiment will demonstrate the feasibility of resupplying orbiting facilities with liquid helium. The SHOOT experiment, designed for transfer rates of 300 to 800 liters/hr, will employ a thermomechanical pump and four screen-covered flow channels for fluid acquisition. The present report centers on cavitation and thermal behavior in ground-based tests of the pump and of a full-sized channel. A model for estimating the temperature profile at the pump inlet is presented. Large temperature increases in this region can significantly degrade the performance of the fountain pump.

INTRODUCTION

The Superfluid Helium On-Orbit Transfer (SHOOT) project is intended as a demonstration of the critical technologies involved in the delivery of liquid helium in a reduced gravity environment.[1] An important component in this process is the fluid acquisition device. The purpose of this device is to ensure that the liquid helium is in contact with the pump inlet at all times during the transfer operation. A number of methods for accomplishing this acquisition have been suggested. The selected method consists of a set of U-shaped screen-covered channels mounted against the dewar wall and joining at the pump inlet. A fountain effect pump has been selected as the device for delivery of the liquid helium in SHOOT. During operation the screen may be partially exposed to helium vapor on the outside of the flow channel. The liquid within the channel may experience pressures below saturation and thus will be contained by the surface tension of the helium.

* current address, Physics Department, Stanford University, Stanford, CA 94305

DESCRIPTION OF EXPERIMENT

The experiment is configured to provide maximum flexibility in operation of the acquisition system while giving a scaled test of the various components involved. A schematic of the entire assembly is shown in Fig. 1. It consists of two He II reservoirs connected by a line containing a fountain pump. The upper reservoir is the receiver dewar which acts as a buffer volume for the transferred helium. The lower reservoir is a horizontally oriented cylinder 0.15 m in diameter and 0.74 m long. It has an enclosed volume of 13 dm^3. Both reservoirs are installed in the Liquid Helium Flow Facility (LHFF) at the University of Wisconsin which provided vacuum insulation and a 4.5 K radiation shield to minimize the heat leak to the experiment.

The lower reservoir contains the fluid acquisition channel. This device was fabricated by Martin-Marietta to specifications consistent with the full-scale SHOOT dewars. It has a total length of 0.74 m with the last 0.13 m inclined to conform to the walls of the SHOOT cryostat. The upper surface of the channel is covered by a fine mesh stainless steel Dutch weave screen with an effective pore size of 5 microns. Flow characteristics and further details of the channel have been presented elsewhere.[2]

In the experiment the temperature is stabilized by regulating the vapor pressure in the receiver dewar. He II is initiated by applying up to 33 watts of power to heater H. The flow rate is determined by measuring the pressure differential across a venturi instrumented with two Siemens KPY-12 pressure transducers. The integrated flow rate is also determined by monitoring the liquid level in the receiver dewar. All data are recorded as a function of time using a computer data acquisition system.

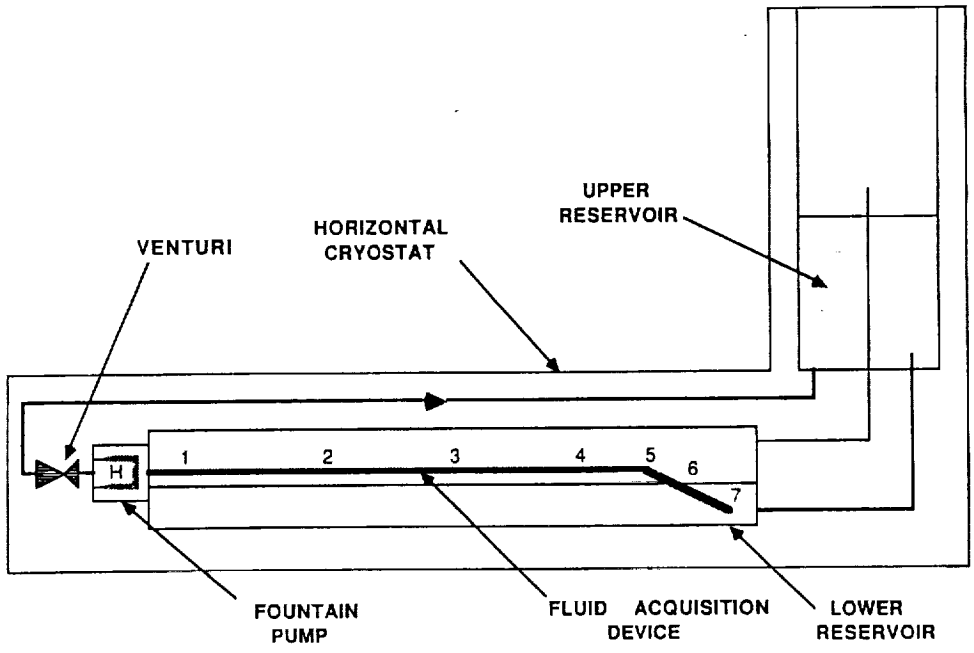

Fig. 1 Schematic of the SHOOT ground test assembly

PRINCIPLE OF OPERATION

When the channel is totally submerged in liquid helium, the liquid flows freely through the screen and is pumped along the channel to the fountain pump. When the screen is partially exposed to vapor, the surface tension of liquid-vapor interface within the pores of the screen prevents the vapor from being ingested into the channel. As long as there is no vapor within the channel, liquid continues to flow through the submerged portion of the screen and is delivered to the fountain pump.

The fluid in the channel can be at a pressure lower than the helium saturated vapor pressure for the ambient liquid temperature. This is a metastable state due to the flow pressure drop. It is energetically favorable for any vapor cavity that is ingested or formed in the channel to grow, returning the fluid to the saturation curve and causing the pump to stop. The pressure inside the channel theoretically can be $2\sigma/r$ (where σ is the surface tension and r is the effective radius of a pore) below the vapor pressure before vapor is ingested through the screen. The pressure at the inlet of the fountain pump is below the vapor pressure by the sum of pressure loss through the screen, a small pressure drop (less than on Pa) due to frictional losses in pumping the fluid along the length of the exposed channel, and the negative gravitational head due to bath level being below the top of the screen.

In addition to the pressure gradient across the screen there will be a temperature gradient established at the pump inlet as entropy is carried by the normal fluid from the fountain pump to the colder bath. The liquid helium in the channel becomes superheated compared to ambient conditions. This effect puts the fluid in the channel even further into the metastable region increasing the potential for formation of vapor at heterogeneous nucleation sites. In order for the SHOOT experiment to be successful, the channel must not cavite from from heating or when it experiences accelerations of as much as $10^{-4} m/s^2$. This is equivalent to pumping against a -0.1 mm head of helium on earth.

TEMPERATURE GRADIENT IN THE CHANNEL

Information on the dynamics of this system can be obtained by examining the temperature at various locations within the channel. Figure. 2 presents the time variation of the temperature at the outlet (upper trace) and inlet to the fountain pump (lower trace) when 2.5 watts of power are applied to the pump heater. Aside from the transient behavior in the first 100 seconds, this occurrent rise in temperature is the sum of two effects: the bath temperature rise due to insufficient pumping power, and the temperature rise in the channel due to the thermal impedance of the screen. Any temperature rise in the channel will result in decreased efficiency of the transfer, and increase in the channel temperature above the bath temperature will superheat the liquid moving it further into the mestastable region. It is therefore important to understand the sources and magnitude of these contributions.

We can readily obtain an approximate solution for the heat flow in the screen lined channel by solving the appropriate heat transport equations. The temperature gradient along the channel may be expressed as

$$\frac{dT}{dx} = f(T)\left(\frac{Q(x)}{wh}\right)^3 \qquad (1)$$

where $f(T)$ is the He II thermal resistance function and Q(x) is the local heat flux. The channel has a width, w = 5.72 cm. and height, h = 1.27 cm. Equation (1) neglects the small contribution resulting from forced convection. Heat transfer through the screen is determined by internal

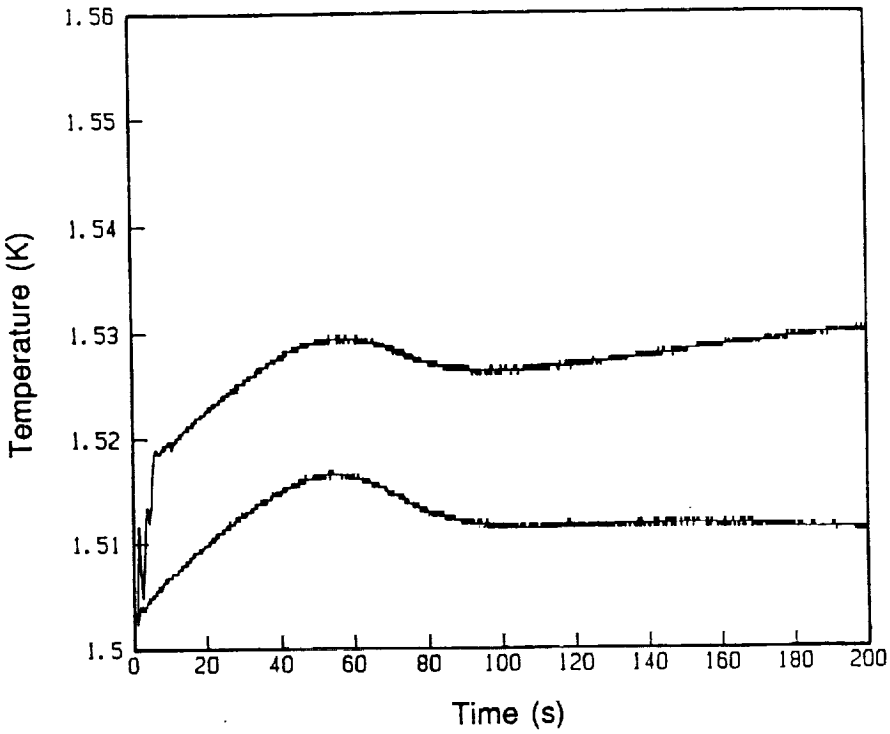

Fig. 2 Temperature at the inlet (lower trace) and outlet (upper trace) of the fountain pump with 2.5 Watts heatings. The screen is totally submerged for the entire trace.

convection within the screen pores. If we assume that turbulent conditions exist, then the heat flux gradient along the channel may be approximated by

$$\frac{dQ(x)}{dx} = \frac{\varepsilon\, w}{f(T)^{1/3}} \left(\frac{T-T_b}{l} \right)^{1/3} \tag{2}$$

where ε is the screen void fraction and l the effective thickness. For the screen material in the present experiment, $\varepsilon = 0.287$ and $l = 98.8$ μm. There is an additional contribution due to internal convection transverse across the channel. This contribution, which is the same form as Equation (2), is neglected for simplicity in the present analysis. Its inclusion would not substantially affect the outcome of the calculations. Combining Equations (1) and (2) we obtain a differential equation which can be solved for the assumed boundary conditions. The temperature profile is exponential,

$$T - T_b = (T_o - T_b) \exp\left(-\frac{x}{\alpha} \right) \tag{3}$$

where T_o is the temperature at the channel inlet. The decay length α, has a value of 4.2 mm for the parameters of the present experiment.

The temperature difference between the pump inlet and the bath is controlled by the total heat applied to the fountain pump. Assuming ideal behavior for the pump,

$$T_o - T_b = \frac{f}{\alpha} \left(\frac{Q_o}{wh} \right)^3 \tag{4}$$

which can be related to the mass flow rate through the thermomechanical expression .[3] The ratio is therefore only a function of temperature, see Figure 3. This result suggests that there can be a

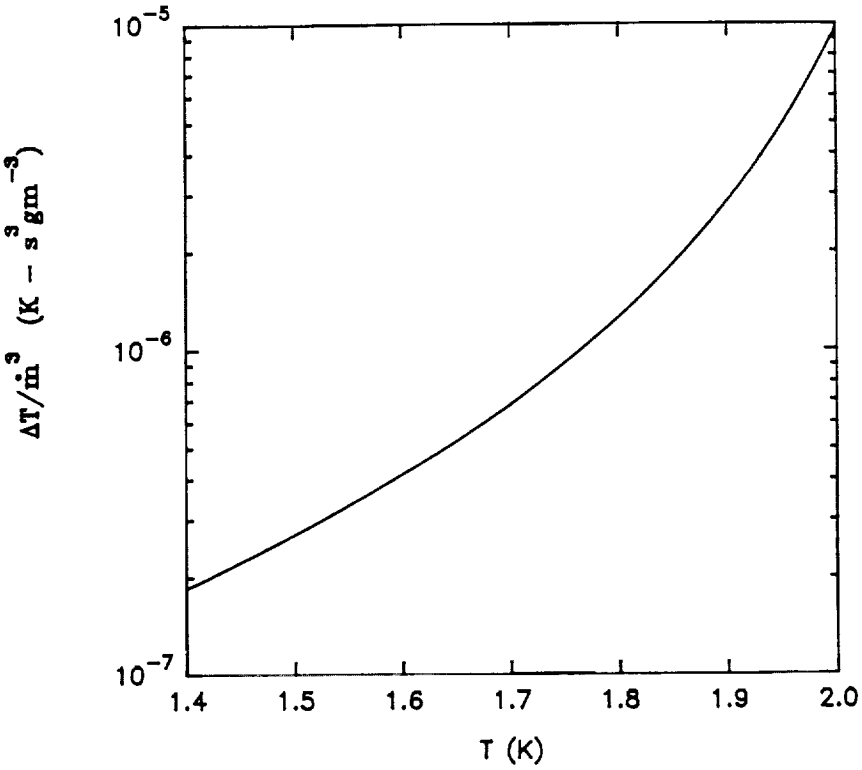

Fig. 3 The calculated ratio $\Delta T/m^3$, across the screen at the inlet of the fountain pump as a function of bath temperature. This figure is valid for $\Delta T << T_b$.

sizable temperature increase at the pump inlet, which will in turn reduce the performance of the pumping system. Listed in Table I are calculated temperature increases for different bath temperatures and heat fluxes. At the highest heat flux, the temperature rise is sufficient to cause cavitation at the pump inlet.

The above calculation predicts a temperature increase for the conditions in Figure 2 of about 0.2 mK. Clearly the observed rise in temperature at the inlet is due to other effects such as insufficient pumping power to remove the heat from the lower reservoir.

The preceding example does not imply that temperature rise at the pump inlet is unimportant to the performance of the SHOOT channel. For example, at a transfer rate of 30 gm/s and a 1.8K bath temperature, the temperature at the inlet will rise about 270 mK, which is sufficient to reduce transfer efficiency and possibly cavitate the pump. The temperature rise will not affect the ingestion of vapor through the screen since this is determined by the pressure difference.

CAVITATION RESULTS

After the experimental run a hole was discovered along the top of the weld joining the channel to the fountain pump. This prohibited the apparatus from reaching the full potential of the screen acquisition system. A bubble test in methanol suggested that the hole was about 50 microns in diameter; thus the channel could only be expected to maintain a pressure differential of about 14 Pa with the hole exposed to vapor. Figure 4 demonstrates that this was indeed the case. In the figure, the volume of helium transferred as measured by the level detector in the upper reservoir is indicated by the monotonically rising line. The transferred volume needed to expose the channel screen is indicated at 4.5 liters. Also plotted in this figure is the temperature at the outlet to the fountain pump. We found the outlet temperature to be a clear indication of cavitation. The cavitation takes place at point A. From point B to point C the reduced flow to the pump caused the outlet temperature to rise until at point C the fluid at the outlet probably boils.

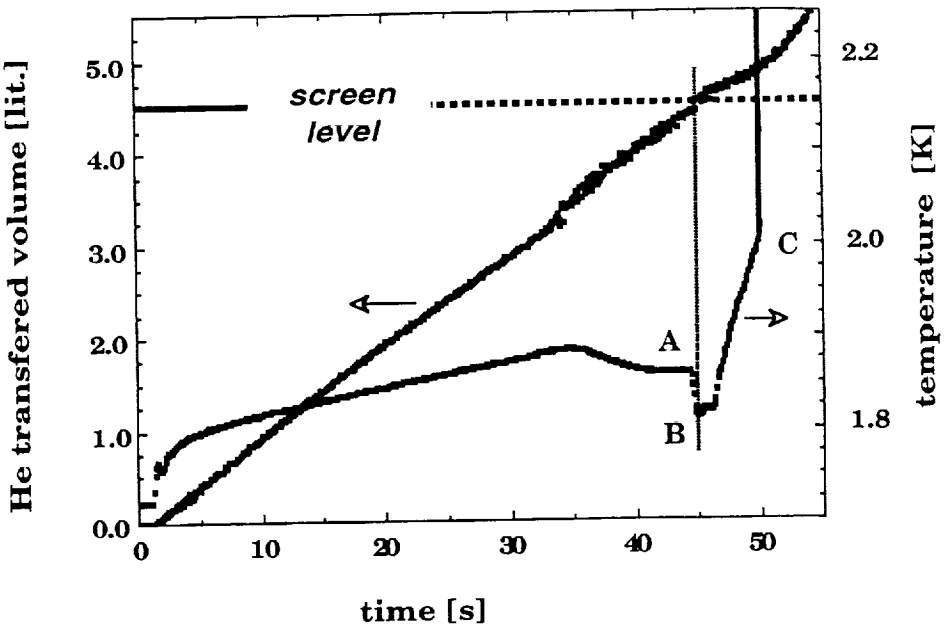

Fig. 4 Ingestion of vapor into the SHOOT acquisition device is indicated by the sudden drop in temperature at the outlet to the fountain pump at point A. The ingestion of vapor is coincident with the liquid level reaching the screen of the gallery arm.

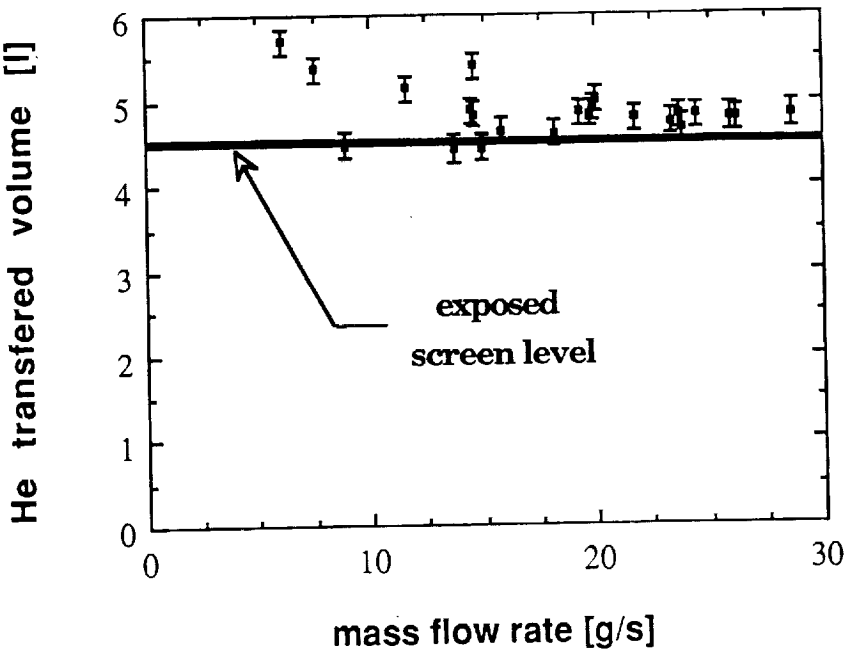

Fig. 5 Level at which vapor was detected versus flow rate.

It is easy to see from this graph that the cavitation takes place simultaneously with the exposure of the 50 micron hole (screen level). Figure 5 summarizes the level at which vapor was detected for a number of trials. These results show that vapor was ingested into the channel when the level dropped more than a few millimeters below the position of the 50 micron hole, in agreement with the bubble point measurement. We also confirmed that the cavitation occurred when the pressure differential was about 14 Pa. Note that there are no signs of vapor formation until the screen is exposed. This result suggests that heterogeneous nucleation of the metastable liquid does not play a significant role for short excursions into the mestatable region.

SUMMARY AND CONCLUSIONS

The temperature gradient predicted in this report was too small to be seen with the instrumentation installed in the test article because the resolution of the thermometers was only ± 1 mK and because they were placed too far from the inlet to the fountain pump (the nearest was 1 cm upstream) to record the predicted exponential decay. The expectation that most of the heat transfer through the screen takes place in the first 5mm from the inlet probably accounts for the unexpectedly large pressure drop measured at the inlet.[2] While the issue of heat transfer is expected to have little impact on the ingestion of vapor into the channel, it could have a profound impact on the heterogeneous nucleation rate if the supply temperature is too high.

ACKNOWLEDGMENTS

Work sponsored by NASA-Goddard Space Flight Center under grant NAG5-1031. Discussions with J. R. Maddocks, Jr. are gratefully acknowledged.

REFERENCES

1. M. J. Di Pirro, Superfluid Helium On-Orbit Transfer Flight Experiment: Performance Estimates, Cryogenics 28: 77 (1988).

2. J. A. Nissen, B. Maytal and S. W. Van Sciver, Pressure Drop in the SHOOT Superfluid Helium Acquisition System, Cryogenics 30: 211 (1990).

3. M. J. DiPirro and R. F. Boyle, Lab Tests of a Thermomechanical Pump for SHOOT, "Advances in Cryogenic Engineering" Vol. 33, Plenum Press, New York (1987) pp. 487.95.